

Effect of Curvature on Three-Dimensional Boundary-Layer Stability

M. R. Malik*

High Technology Corporation, Hampton, Virginia

and

D. I. A. Poll†

Cranfield Institute of Technology, Cranfield, England, U. K.

The problem of the stability of a three-dimensional laminar boundary layer formed on a curved surface is considered. A calculation scheme, which takes account of the curvature of the flow streamlines and of the surface, is proposed for the prediction of the development of small-amplitude temporal disturbances. Computations have been performed for the flow over the windward face of an infinitely long yawed cylinder and comparisons have been made with experimental data. These indicate that the theory correctly predicts many of the features of the unstable laminar flow. The theory also suggests that transition, in this particular situation, is dominated by traveling disturbance waves and that, at the experimentally observed transition location, the wave which has undergone the greatest total amplification has an amplitude ratio of approximately e^{11} . When the effects of curvature are omitted, the maximum amplitude ratio of the transition is about e^{17} .

Nomenclature

A	= disturbance amplitude
a	= leading-edge radius of cylinder model
C	= chord length of cylinder model measured in a plane normal to the leading edge
c	= velocity component in the η direction
f	= disturbance frequency, Hz
$g_{1,2}$	= metric coefficient for the x, y, z system of axes
$h_{1,2}$	= metric coefficients for the ξ, η, ζ system of axes
N	= logarithmic exponent of disturbance amplitude ratio ($e^N = A/A_0$)
p	= static pressure
Q	= total flow velocity, $(u^2 + v^2)^{1/2}$
r	= radial coordinate in the cylindrical polar system r, θ, ζ
R_c	= freestream Reynolds number ($Q_\infty C/\nu$)
s	= velocity component in the ξ direction
t	= time
T_u	= turbulence level, $[\frac{1}{2}(\tilde{u}^2 + \tilde{v}^2 + \tilde{w}^2)/Q_\infty^2]^{1/2}$
U_0	= boundary-layer reference velocity
u, v, w	= velocity components inside the boundary layer in the x, y, z directions
x, y, z	= set of fixed reference axes (Fig. 1)
α, β	= real disturbance wavenumber in the ξ and η directions, respectively
δ	= boundary-layer reference length
ϵ	= angle between x and ξ coordinate directions
η	= coordinate direction in the wave aligned ξ, η, ζ system
θ	= azimuthal coordinate in the cylindrical polar system r, θ, ζ (Fig. 1)
Λ	= cylinder leading-edge yaw angle
λ	= wavelength of stationary disturbances
ν	= kinematic viscosity
ξ	= coordinate direction in the wave-aligned ξ, η, ζ system (Fig. 1)

ϕ	= angle between the wavenumber vector and the ξ direction
ψ	= angle between the external streamline direction and the x direction (Fig. 2)
ω	= complex disturbance frequency
ζ	= axial component in the cylindrical polar coordinate system r, θ, ζ

Superscripts

$(\bar{\quad})$	= mean (time averaged) quantity
$(\hat{\quad})$	= fluctuating quantity
$(\hat{\quad})$	= disturbance amplitude function
$(\quad)'$	= differentiated with respect to z

Subscripts

e	= at the edge of the boundary layer
i	= imaginary part of a complex number
r	= real part of a complex number
∞	= in the undisturbed freestream

Introduction

THE rapid increases in the cost of fossil fuels over the past decade have provided a very strong incentive for the development of a new generation of energy-efficient transport aircraft. There are several aspects of aircraft aerodynamic design that, with varying degrees of technological development, could lead to significant reductions in cruise drag.¹ However, of the various options available, laminar flow control (LFC) offers the greatest potential for improved aerodynamic efficiency. Unfortunately, at the Reynolds numbers typically encountered in long-range cruise, the boundary-layer flows formed on the wings of aircraft in current service are usually turbulent right from the leading edge. Consequently, the establishing and maintaining of laminar boundary layers under such conditions requires a quantum jump in wing design methods and in related systems, materials, manufacturing and operating technologies. It follows that success or failure in such a "high-risk," long-term venture depends crucially on our understanding of the physics of laminar flow stability and, in particular, on our ability to predict those conditions for which laminar flow is no longer viable.

Received May 14, 1984; presented as Paper 84-1672 at the AIAA 17th Fluid Dynamics, Plasma Dynamics and Lasers Conference, Snowmass, CO, June 25-27, 1984; revision received Oct. 5, 1984. Copyright © American Institute of Aeronautics and Astronautics, Inc., 1985. All rights reserved.

*President, Member AIAA.

†Lecturer in Aerodynamics, Aerodynamics Division, College of Aeronautics, Member AIAA.

At present, the "state-of-the-art" transition prediction method involves the use of linear stability theory coupled with an e^N breakdown criterion. This particular method was originally proposed by Smith (see Ref. 2), who showed that for transition in two-dimensional and axisymmetric flow the N factor takes a value of about 10 when the freestream disturbance levels are small ($T_u < 0.15\%$). The extension of the method to three-dimensional flows is not entirely straightforward since the extra degree of freedom means that there are several ways to calculate an N factor from the stability characteristics. The envelope³ and saddle point^{4,5} methods are two such alternative approaches. However, it has been demonstrated by Malik and Orszag⁶ that, for a given case, the ultimate values of N are only very weakly dependent upon the approach adopted. Given this, it would appear that a three-dimensional version of the e^N procedure may have a useful role as a design tool if it can be demonstrated that the N factor is still equal to 10 when the computations are compared with transition data from fully three-dimensional experiments. Initial attempts to provide the necessary "proof" have been carried out by Hefner and Bushnell,⁷ who used the SALLY code of Srokowski and Orszag³ to analyze a series of transition experiments performed on swept-back wing configurations. On the basis of the few experimental situations available to them, they concluded that the N factor at transition was between 7 and 11. However, when Cebeci and Stewartson⁵ applied the method to the problem of flow over a rotating disk, the N factor at transition was found to be about 20.

The SALLY code and the code used by Cebeci and Stewartson⁵ derive the stability characteristics from solutions of the Orr-Sommerfeld equation. This classical stability equation is obtained from the time-dependent Navier-Stokes equation for the perturbed flow by way of several important physical assumptions. For the three-dimensional stability problem, Stuart⁸ has shown that, in general, the stability of the flow is affected by curvatures of the body surface and also of the flow in planes drawn parallel to the surface, plus the Coriolis forces if the body is rotating. Therefore, if the Orr-Sommerfeld equation is to provide reliable stability data, the contributions from these extra terms must be negligibly small in comparison with those from the retained terms. Since there is no a priori formal justification for excluding the curvature and Coriolis effects from the stability analysis for the rotating disk problem, Malik, Wilkinson, and Orszag⁹ performed computations in which these effects were included. Their results showed that these terms had a powerful stabilizing effect and that the contribution of flow curvature in planes parallel to the surface was particularly important. Moreover, the revised analysis showed that the experimentally observed transition point corresponded to an N factor of 11.

The results of Malik et al.⁹ have important implications for the prediction of transition near the leading edge of a swept-back wing (or yawed cylinder). In this region, both the surface and the flow streamlines are highly curved. The curvature of the streamlines leads to the development of a "cross-flow" velocity component within the boundary layer, and the velocity profiles associated with the cross flow are known to exhibit instability at low Reynolds numbers (e.g., see Refs. 7 and 10). Despite the fact that cross-flow instability has long been recognized as a major transition-inducing mechanism on swept wings, the effect of the streamline curvature on the stability characteristics has never been addressed. We also note that none of the swept-wing examples considered by Hefner and Bushnell⁷ involved transition in regions of high curvature and so their rather tentative conclusions cannot be expected to be globally valid—particularly in view of the rotating disk experience.

The object of the present paper is to present a method for calculating the stability characteristics of a flow having curvatures of both the surface and the streamlines. Computa-

tions are presented for the case of the flow over the windward face of an infinitely long yawed cylinder. This is known to be a situation in which the transition process is governed by the instability of the curvature-induced cross flow and, consequently, it provides an excellent test case for the extended stability analysis. Finally, the predictions are compared with experimental measurements made on a cylinder model in a low-speed wind tunnel with a low freestream turbulence level.

Analysis

We begin by considering the three-dimensional flow over a curved surface and we define two sets of orthogonal curvilinear coordinate systems as indicated in Fig. 1. The first (x , y , and z) is a set of reference axes that remain fixed relative to the body with x and y lying in the plane of the surface and z being normal to the surface. Since these are, in general, curved axes, elements of length in the x , y , and z directions are given by $g_1 dx$, $g_2 dy$, and dz . Therefore, a general element of length dl is given by

$$dl = [(g_1 dx)^2 + (g_2 dy)^2 + (dz)^2]^{1/2}$$

The velocity components u , v , and w are assigned to the x , y , and z coordinate directions. A second set of curvilinear coordinates (ξ , η , and z) is then defined. In this case, the ξ and η coordinates lie in the plane of the surface. Elements of length in this system are $h_1 d\xi$, $h_2 d\eta$, and dz , respectively. Therefore, a general element of length is

$$dl = [(h_1 d\xi)^2 + (h_2 d\eta)^2 + (dz)^2]^{1/2}$$

The velocity components in the ξ and η directions are s and c , respectively. This system of coordinates is used for the stability analysis and is free to rotate relative to the x, y, z system. The angle between the ξ and x axes is ϵ .

Consider a flow where the instantaneous values of velocity and pressure may be expressed in terms of a steady mean component and a fluctuating component,

$$(s, c, w, p) = (\bar{s}, \bar{c}, \bar{w}, \bar{p}) + (\tilde{s}, \tilde{c}, \tilde{w}, \tilde{p})$$

We now assume that the fluctuating components may be described by a very weak harmonic disturbance wave that makes an angle ϵ with the x coordinate direction and we specify that the wave amplitude is a function of time only, i.e.,

$$(\tilde{s}, \tilde{c}, \tilde{w}, \tilde{p}) = \text{Re} \{ (\hat{s}, \hat{c}, \hat{w}, \hat{p}) \exp i(\alpha \xi - \omega t) \}$$

where α is a real wavenumber and ω a complex frequency. The equations governing the temporal stability of a wave whose wavenumber vector is tangent to one of the coordinate axes (ξ) in an orthogonal curvilinear system (ξ, η, z) have already been derived by Stuart.⁸ However, in a given problem, the geometric properties of the disturbance wave are not known at the beginning of the computation. Therefore, it is necessary to develop an iterative scheme for the solution of Stuart's basic equations.

The process begins by considering an initial orientation for the ξ, η, z system relative to x, y, z —say ϵ_1 . We then consider a wave of the form

$$(\tilde{s}, \tilde{c}, \tilde{w}, \tilde{p}) = \text{Re} \{ (\hat{s}, \hat{c}, \hat{w}, \hat{p}) \exp i(\alpha \xi + \beta \eta - \omega t) \}$$

where α and β are real wavenumbers in the ξ and η directions. For this wave, we note that the wavenumber vector makes an angle ϕ with the ξ axis such that

$$\tan \phi = \beta / \alpha \quad (1)$$

In the present analysis, we follow the authors of Refs. 2, 3, and 5-7 and continue to neglect the contribution from the nonparallel terms. Therefore, the equations governing the disturbance behavior in the ξ, η, z system of coordinates are

$$i(\alpha_0 \hat{s} + \beta_0 \hat{c} - \omega) \hat{s} + \hat{s}' \hat{w} + m_{12} (\hat{s} \hat{c} + \hat{c} \hat{s}) - 2m_{21} \hat{c} \hat{c} + m_{13} \hat{s} \hat{w} = -i\alpha_0 \hat{p} + (1/R) [\hat{s}'' - (\alpha_0^2 + \beta_0^2) \hat{s}] \quad (2a)$$

$$i(\alpha_0 \hat{s} + \beta_0 \hat{c} - \omega) \hat{c} + \hat{c}' \hat{w} - 2m_{12} \hat{s} \hat{s} + m_{21} (\hat{s} \hat{c} + \hat{c} \hat{s}) + m_{23} \hat{c} \hat{w} = -i\beta_0 \hat{p} + (1/R) [\hat{c}'' - (\alpha_0^2 + \beta_0^2) \hat{c}] \quad (2b)$$

$$i(\alpha_0 \hat{s} + \beta_0 \hat{c} - \omega) \hat{w} - 2m_{13} \hat{s} \hat{s} - 2m_{23} \hat{c} \hat{c} = -\hat{p}' + (1/R) [\hat{w}'' - (\alpha_0^2 + \beta_0^2) \hat{w}] \quad (2c)$$

and

$$i(\alpha_0 \hat{s} + \beta_0 \hat{c}) + \hat{w}' + m_{12} \hat{c} + m_{21} \hat{s} + (m_{13} + m_{23}) \hat{w} = 0 \quad (2d)$$

The boundary conditions are

$$\begin{aligned} \hat{s} = \hat{c} = \hat{w} = 0 & \quad \text{at } z = 0 \\ \hat{s} \rightarrow 0, \quad \hat{c} \rightarrow 0, \quad \hat{w} \rightarrow 0 & \quad \text{as } z \rightarrow \infty \end{aligned} \quad (2e)$$

In this system of equations, all the variables have been non-dimensionalized with an appropriate boundary-layer velocity U_0 and a reference length scale δ . Both these quantities are assumed to be local constants. The "in-plane" curvature coefficients are given by

$$m_{12} = \frac{\delta}{h_1 h_2} \frac{\partial h_1}{\partial \eta} \quad \text{and} \quad m_{21} = \frac{\delta}{h_1 h_2} \frac{\partial h_2}{\partial \xi}$$

while the surface curvature coefficients are given by

$$m_{13} = \frac{\delta}{h_1} \frac{\partial h_1}{\partial z} \quad \text{and} \quad m_{23} = \frac{\delta}{h_2} \frac{\partial h_2}{\partial z}$$

Finally,

$$\alpha_0 = \alpha/h_1, \quad \beta_0 = \beta/h_2$$

and the Reynolds number used in the stability analysis is

$$R = U_0 \delta / \nu$$

where ν is the kinematic viscosity.

These are general equations governing the quasiparallel stability of three-dimensional boundary layers and, clearly, an application to a specific problem requires the determination of the various curvature coefficients. It may also be readily shown that, if these coefficients are set to zero, then Eqs. (2) can be reduced to the familiar Orr-Sommerfeld equation. Assuming that the necessary curvature coefficients are available, a solution is obtained by specifying the frequency of the disturbance ω , and then determining the values of α and β by requiring that, at any point on the surface, the temporal amplification rate ω_i is maximized at a fixed Reynolds number. This procedure is known as the "envelope" method and is the same as that used by Malik et al.⁹ for the rotating disk problem. Having obtained a first estimate for the shape of the disturbance wave everywhere in the x, y, z space, a new set of ξ, η, z coordinates is specified in such a way that the ξ coordinate is locally aligned with the wavenumber vector, i.e.,

$$\epsilon_2 = \epsilon_1 + \phi \quad (3)$$

The stability characteristics are then recomputed. This process is repeated until ϕ [see Eq. (1)] is effectively reduced to zero. In this event, the solution of Eqs. (2) is also a solution of Stuart's⁸ disturbance equations (with the nonparallel flow terms set to zero) and the stability characteristics then include all the effects of streamline and surface curvature.

Method of Solution of the Governing Equations

Several methods are available for solving the governing linear stability equations. First, these equations can be represented by a coupled system of fourth- and second-order differential equations that can be solved by the Chebyshev spectral-tau approach used in Ref. 9. Alternatively, the governing equations could be reduced to a system of six first-order equations, and then the compact difference scheme described by Malik, Chuang, and Hussaini¹¹ can be employed for the efficient solution of the eigenvalue problem. Due to the nature of calculations needed to generate the coordinate axes, it appeared convenient to adopt an existing compressible stability analysis computer code (COSAL) for the present study.¹² Indeed, the code required only minor changes in order to perform the calculations reported in this paper. A brief description of the numerical method is given below. The governing stability equations are represented as

$$(FD^2 + GD + H)T = 0 \quad (4)$$

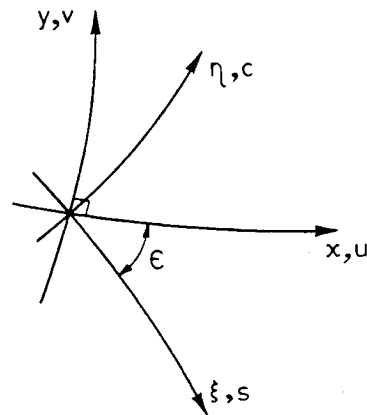


Fig. 1 Notation for the fixed reference and wave aligned systems of orthogonal curvilinear coordinates.

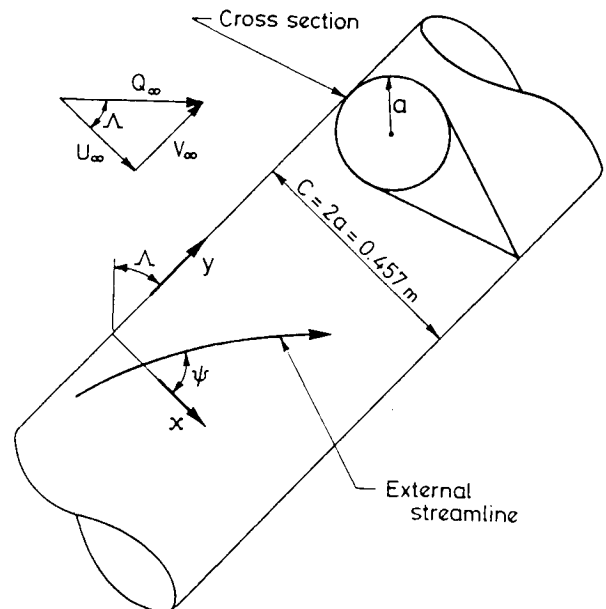


Fig. 2 Notation for the infinitely long yawed cylinder test case.

where T is a four-element vector defined by

$$T = \begin{bmatrix} \hat{s} \\ \hat{w} \\ \hat{p} \\ \hat{c} \end{bmatrix}$$

Here F, G, H are 4×4 matrices and $D \equiv d/dz$. The nonzero elements of the matrices F, G, H are

$$\begin{aligned} F_{11} &= 1 & H_{22} &= \chi \\ F_{22} &= 1 & H_{24} &= +2m_{23}R\bar{c} \\ F_{44} &= 1 & H_{31} &= i\alpha_0 + m_{21} \\ G_{23} &= -R & H_{32} &= m_{13} + m_{23} \\ G_{32} &= 1 & H_{33} &= \gamma \\ H_{11} &= \chi - m_{12}R\bar{c} & H_{34} &= i\beta_0 + m_{12} \\ H_{12} &= -R\bar{s}' - m_{13}R\bar{s} & H_{41} &= 2m_{12}R\bar{s} - m_{21}R\bar{c} \\ H_{13} &= -i\alpha_0R & H_{42} &= -R\bar{c}' - m_{23}R\bar{c} \\ H_{14} &= -m_{12}R\bar{s} + 2m_{21}R\bar{c} & H_{43} &= -i\beta_0R \\ H_{21} &= +2m_{13}R\bar{s} & H_{44} &= \chi - m_{21}R\bar{s} \end{aligned}$$

where

$$\chi = -iR(\alpha_0\bar{s} + \beta_0\bar{c} - \omega) - \alpha_0^2 - \beta_0^2$$

and γ is a small artificial compressibility parameter. The parameter γ was introduced to solve the governing equations (2) using COSAL and it was assigned a value of 10^{-13} . Tests were conducted to investigate the dependence of the physical results upon the value of γ . However, no direct dependence was observed.

The system of Eq. (4) is discretized on a staggered finite difference grid where the velocity perturbations are defined on the cell faces and pressure perturbation on the cell centers. In this way, no pressure boundary conditions are required. Homogeneous velocity perturbation boundary conditions are imposed at the solid boundary ($z=0$) and in the freestream (which is assumed to be at $z=100$). The governing equations, along with the boundary conditions, then result in a block-tridiagonal system of equations with 4×4 blocks that is solved using fully pivoted LU factorization. The eigenvalue ω is obtained by inverse Rayleigh iteration procedure,¹³ which has cubic convergence. For a fixed physical frequency ω_r , the COSAL code calculates the maximum temporal growth rate ω_i , which then determines α and β . The group velocity $V_g = (\partial\omega/\partial\alpha, \partial\omega/\partial\beta)$, which is needed in this maximization procedure and for converting temporal growth to spatial growth, is also calculated in COSAL. More details of the numerical method are given by Malik and Orszag.¹⁴

An N factor for transition correlation purposes may be defined as

$$N = \int_{\ell_0}^{\ell} \omega_i / |\text{Re}(V_g)| d\ell$$

where ℓ is the arclength on the solid body along a curve that is everywhere tangent to $\text{Re}(V_g)$.

Computations for a Yawed Cylinder Configuration

In order to test the method described in the previous section, computations have been performed for the flow over the windward face of the infinitely long yawed cylinder shown in Fig. 2. The natural choice for the fixed-reference axes in this case is the cylindrical polar system r, θ, ζ . For the body-fixed system of Fig. 2, we note that on the windward face

$$x = a\theta, \quad y = \zeta, \quad \text{and} \quad z = r - a$$

where a is the leading edge radius of the cylinder. Hence, by considering the length of a small element, it follows that

$$g_1 = 1 + (z/a) \quad \text{and} \quad g_2 = 1$$

The mean boundary-layer flow was computed, in this coordinate system, from an experimentally determined surface pressure distribution¹⁵ by using a laminar, compressible, adiabatic wall method known as MAIN.¹⁶ For the stability computations, the reference velocity U_0 and reference length δ were chosen to be the boundary-layer edge velocity and the displacement thickness in the x direction. Since these scales are treated as local constants, any other choice of the scales will do equally well. The general form for the curvature coefficients in Eqs. (2) is then

$$m_{12} = \frac{\delta}{h_1 h_2} \frac{\partial h_1}{\partial \eta} = k \cos \epsilon \frac{d\epsilon}{dx}$$

$$m_{21} = \frac{\delta}{h_1 h_2} \frac{\partial h_2}{\partial \xi} = -k \sin \epsilon \frac{d\epsilon}{dx}$$

$$m_{13} = \frac{\delta}{h_1} \frac{\partial h_1}{\partial z} = \frac{k \cos^2 \epsilon}{(1 + kz)}$$

and

$$m_{23} = \frac{\delta}{h_2} \frac{\partial h_2}{\partial z} = \frac{k \sin^2 \epsilon}{(1 + kz)}$$

where $k = \delta/a$. Note that x has been nondimensionalized with respect to a , and z with respect to δ .

Since, on the basis of previous experience,¹⁰ the most unstable disturbances were expected to lie close to the "cross-flow" direction, i.e., in a direction normal to that of the flow at the edge of the boundary layer, the initial ξ, η, z coordinate direction was chosen so that the η direction was aligned with that of the local external streamline. Therefore, the initial orientation is obtained by setting $\epsilon = \pi/2 - \psi$; i.e.,

$$m_{12} = k \tan \Lambda \sin \psi \cos^2 \psi \frac{f'(x)}{f^2(x)} \quad (\text{streamline divergence})$$

$$m_{21} = -k \tan \Lambda \cos^3 \psi \frac{f'(x)}{f^2(x)} \quad (\text{streamline curvature})$$

$$m_{13} = \frac{k \sin^2 \psi}{(1 + kz)} \quad (\text{surface curvature in } \xi \text{ direction})$$

$$m_{23} = \frac{k \cos^2 \psi}{(1 + kz)} \quad (\text{surface curvature in } \eta \text{ direction})$$

where $f(x) = U_e/U_\infty$ and ψ is the angle between the external streamline and the x direction,

$$\tan \psi = \frac{V_e}{U_e} = \frac{V_\infty}{U_\infty f(x)} = \frac{\tan \Lambda}{f(x)}$$

This system of coordinates proved to be an entirely satisfactory starting point for the present problem, with convergence being complete after four iterations through Eq. (3).

Solutions have been obtained for the combinations of sweep angle Λ and freestream Reynolds number R_c shown in Table 1.

The computations for each of these cases showed similar trends and, therefore, detailed results are presented for case 4 only. These are given in Figs. 3-6. Figure 7 shows a summary of the variation of N_{\max} with surface position for cases 1-3. One particularly interesting feature of the yawed cylinder flow concerns the relevance of the stationary disturbances to the stability problem. The existence of such disturbances was first noted by Gray,¹⁷ who observed them while performing transition studies on swept-wing aircraft in flight. Subsequent investigations¹⁵ conducted on wings in wind tunnels have confirmed that the existence of stationary disturbances in the laminar flow regime is a characteristic feature of cross-flow instability. In the present analysis, the stationary disturbances correspond to those waves for which $\omega_r(f)$ is zero. For test case 4, the results presented in Fig. 3 indicate that the stationary wave is unstable and the variation of its wavelength and wavenumber vector orientation are presented in Figs. 8 and 9, respectively.

Discussion

The results presented in Figs. 3-6 indicate that, in the case of the flow over the windward face of a yawed cylinder, curvature has a significant effect upon the flow stability. For a disturbance of fixed frequency, the wavenumber and orientation of the wavenumber vector are modified slightly; however, the most significant change occurs in the amplification rate ω_r . The curvature terms are found to produce a very strong damping effect. This is consistent with the findings of Malik et al.⁹ for the case of a rotating disk. The reduced local amplification rate causes a dramatic reduction in the value of the local N factor for the various unstable disturbance frequencies, as shown in Fig. 3. For this case, N is approximately halved for values of x/C in excess of 0.15. The results presented in Fig. 3 have two other significant features. First, for a fixed value of the freestream Reynolds number, the frequency that has undergone the greatest total amplification (largest N) at a given location is the same (1000 Hz) for all values of x/C lying between 0.1 and 0.31. This is different from the situation normally encountered in two-dimensional flow, e.g., the Blasius boundary layer, where the frequency exhibiting the local maximum N factor decreases monotonically with increasing downstream distance x/C . The second significant feature is that, in the yawed cylinder case, the most highly amplified wave at a given position is, in general, a traveling wave (see Fig. 7). This contrasts with the rotating disk case where Malik et al.⁹ found that the stationary disturbances gave the highest N factor over all of the positive real frequencies. Therefore, it is not at all clear whether the stationary disturbances actually play a significant role in the ultimate breakdown of the laminar flow.

The stability of the boundary layer formed on the windward face of a cylinder with the same geometry as that sketched in Fig. 2 has been investigated experimentally by Poll¹ and a comprehensive description of the procedure and the results is given in Ref. 15. Briefly, the tests were con-

ducted on a model with a chord length C of 0.457 m set at angles of 53-71 deg to the oncoming flow. The wind tunnel was capable of providing freestream speeds in the range of 7.5-55 m/s with a freestream turbulence level T_u of better than 0.16%. Experimental data were obtained for the conditions necessary for the appearance of stationary disturbances in surface evaporation and surface oil flow visualization patterns, the pitch (wavelength) of the disturbances, and the orientation of the disturbances relative to the x axis. Data were also obtained for the frequencies of naturally occurring time harmonic disturbances and the conditions necessary for transition onset.

With regard to the stationary disturbances, the observations made at the conditions corresponding to the case 4 computations have been added to Figs. 8 and 9. It is apparent that the experiment and theory are in reasonable agreement. For the disturbance wavelength, the discrepancy

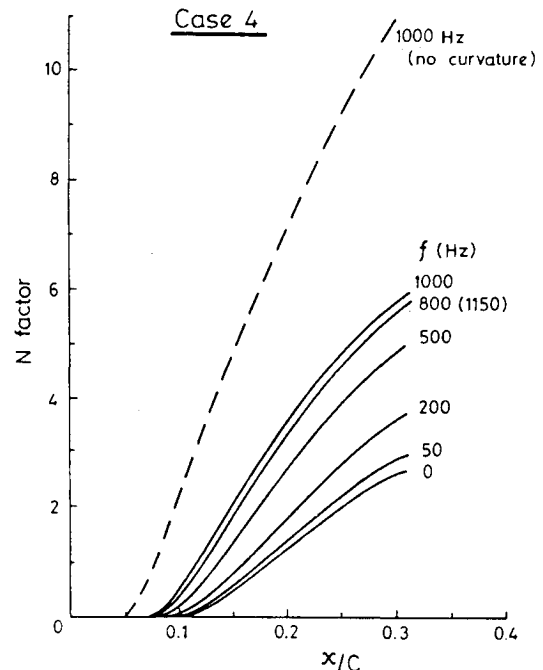


Fig. 3 N factor variation with position and disturbance frequency for a flow with a fixed freestream Reynolds number.

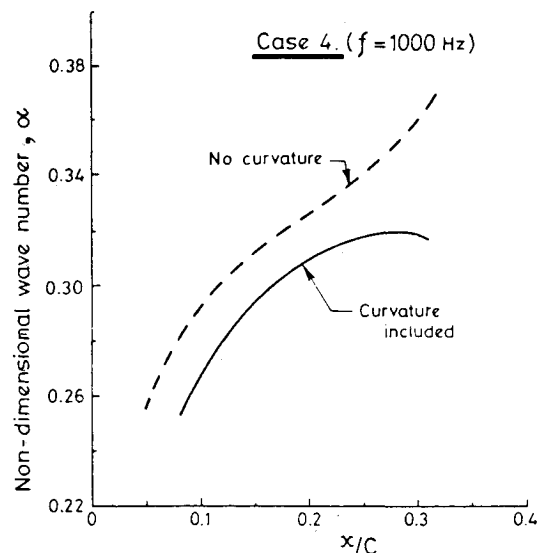


Fig. 4 Disturbance wavenumber as a function of position for a wave of fixed frequency and a constant freestream Reynolds number.

Table 1 Combinations of sweep angle and R_c

Case No.	Λ , deg	$R_c \times 10^{-6}$
1	30	3.81
2	55	1.68
3	60	1.34
4	63	0.88

is less than 10% and for the wavenumber orientation the difference is of order 2 deg. It should also be noted that the stationary disturbances are found to lie at a fixed angle relative to the pure cross-flow direction. The present theory suggests that this angle is approximately 4 deg, while the observations indicate an angle of about 6 deg. These results support the original suggestion made by Owen and Randall¹⁰ and Gregory, Stuart, and Walker⁸ that the stationary disturbances are associated with a velocity profile for which a point of inflection coincides with a point of zero mean velocity. This is the so-called "critical profile" and mean flow computations reveal that, in the present case, this profile makes an angle of 5 deg with the cross-flow direction. In the experiment, time-dependent disturbances were investigated by the use of hot wires placed at fixed locations in the flow. An example relevant to the case 4 computations is presented in Fig. 10. This is an oscilloscope trace showing the fluctuating components of the signals from a pair of hot-wire probes. The cylinder is yawed at 63 deg and the freestream Reynolds number is 0.9×10^6 . In the figure, the upper trace comes from a probe fixed at an x/C of 0.31, while the lower trace shows the response of a probe in the

attachment-line flow ($x/C=0$). The attachment-line trace shows no sign of perturbation at this Reynolds number, but at an x/C of 0.31 strong time harmonic disturbances are present. This disturbance has a very clearly defined frequency of approximately 1050 Hz. Referring to the computations given in Fig. 3, it is clear that at the attachment line ($x/C=0$) no instability is predicted, for x/C greater than 0.1 a stationary disturbance is amplified, but at an x/C of 0.31 the wave that has undergone the greatest total amplification is a traveling one with a frequency of 1000 Hz. Clearly, the

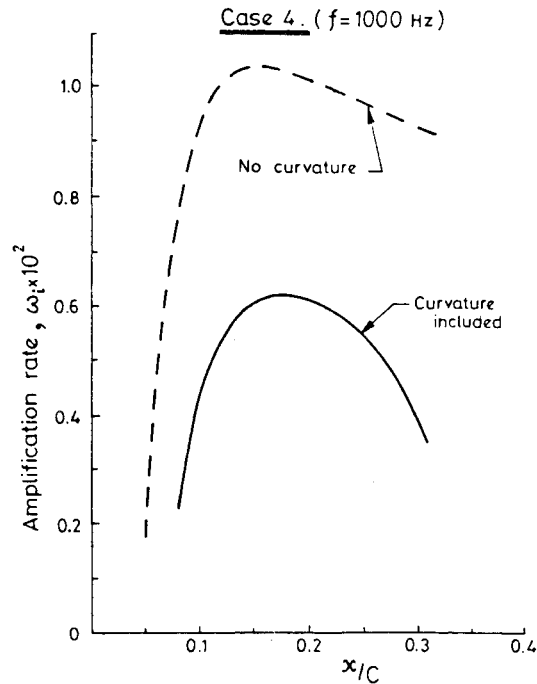


Fig. 5 Temporal amplification rate as a function of position for a wave of fixed frequency and a constant freestream Reynolds number.

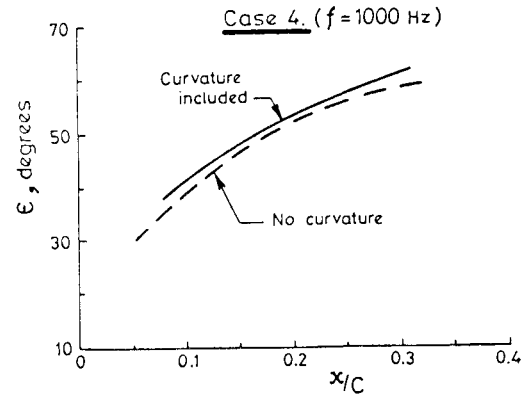


Fig. 6 Orientation relative to the x direction for a wave of fixed frequency and a constant freestream Reynolds number.

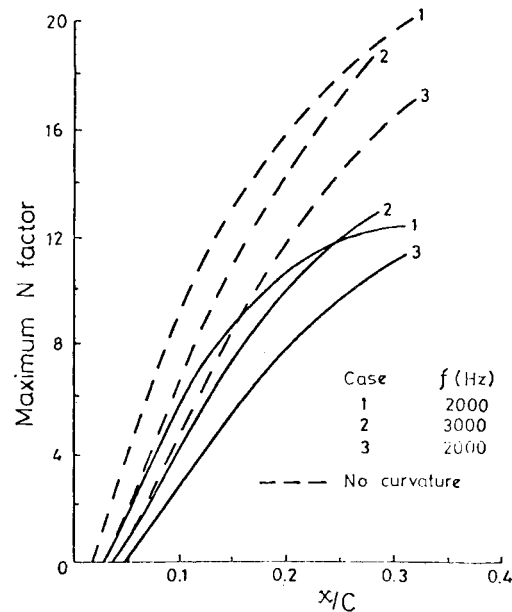


Fig. 7 Variation of the maximum N factor with position for cases 1-3.

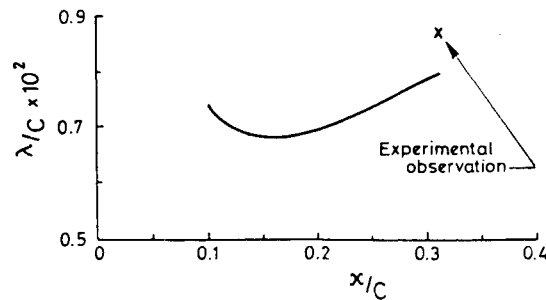


Fig. 8 Variation of the stationary disturbance wavelength with position for the case 4 conditions.

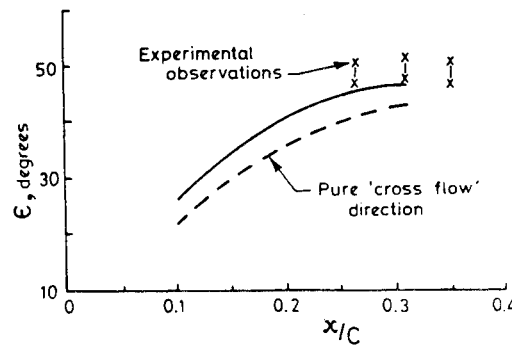


Fig. 9 Stationary disturbance wave orientation relative to the x coordinate direction for the case 4 conditions.

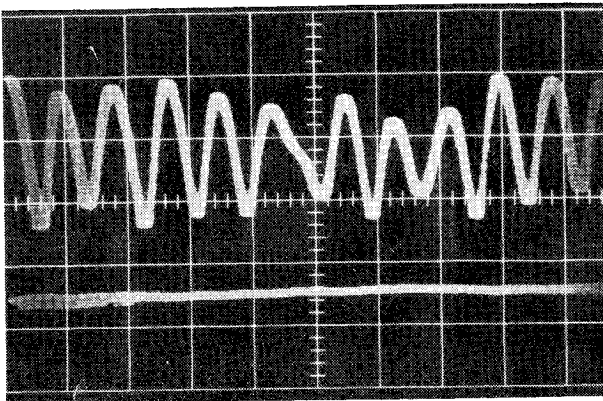


Fig. 10 Oscilloscope trace showing the velocity fluctuations in the unstable laminar flow (yaw is 63 deg and the freestream Reynolds number is 0.9×10^6). Upper trace shows condition of $x/C=0.31$, lower trace shows condition of $x/C=0$. Vertical scale is 0.1 V/large division and time base is 1 ms/large division.

agreement between the predictions and the limited observations for the instability of the laminar layer is very good.

As stated previously, the main engineering objective of stability computations is the prediction of the location of the onset of the boundary-layer transition. In two-dimensional flows, the current criterion² is simply that transition begins at that point in the flow where the N factor for any fixed frequency disturbance just reaches 10. Therefore, it is interesting to examine the relevance of this criterion to the highly three-dimensional flow on the yawed cylinder. The experiment provides transition onset data for the computational cases 2 and 3. At these flow conditions, the surface Pitot-tube technique indicates that transition begins at an x/C of 0.26 and 0.31, respectively. From Fig. 7 it can be seen that for the computations including the effects of curvature, the N factors at transition are 12.3 and 11.2. These are in excellent agreement with the value of 11 obtained by Malik et al.⁹ for transition onset on the rotating disk and they lie well within the uncertainty bounds for N at the transition onset in two-dimensional flows as reported by Jaffe et al.² However, when the curvature effects are omitted, the values of N at transition are found to be 17.7 (case 2) and 16.9 (case 3). It is apparent that the use of the Orr-Sommerfeld equation for generating stability characteristics for use in the prediction of transition onset on the cylinder is totally inappropriate and that this approach, coupled with the conventional " N equals 10" criterion, would yield extremely pessimistic transition locations.

Finally, it should be noted that for cases 2-4 the yaw angles are relatively large, being 55, 60, and 63 deg, respectively. Since these angles are considerably greater than those occurring at the leading edges of typical civil transport aircraft, it is appropriate to examine the effects of curvature on the cylinder flow at a much smaller yaw angle. This problem is addressed in computational case 1 where the yaw angle is only 30 deg. The predicted variation of N factor with x/C is given in Fig. 7. These results indicate that the damping effects of the curvature terms are still strong at the reduced yaw angle. Moreover, the most highly amplified disturbance is a traveling wave with a frequency of 2000 Hz. Therefore, there would seem to be no indication that the stationary disturbances are any more important in this case than they are at the large yaw angles. By assuming an N factor of between 11.2 and 12.3 for transition onset, it is apparent that for case 1, transition onset should occur between an x/C of 0.23 and 0.31. At approximately 60 deg yaw, transition occurred in this region when the freestream Reynolds number was about 1.5×10^6 , while at 30 deg the Reynolds number required is 3.8×10^6 . This comparison clearly demonstrates the strong destabilizing effect of yaw.

Conclusions

The effects of curvature on the stability of a three-dimensional laminar boundary layer have been studied theoretically. A scheme has been proposed for the computation of the linear stability characteristics of fixed-frequency, temporal, disturbance waves and sample computations have been performed for the case of the flow over the windward face of a long yawed cylinder. These computations have shown that in this case the body curvature and streamline curvature terms produce strong damping effects, together with significant changes in the magnitude and orientation of the wavenumber vector. Comparison with the experimental data available for this flow indicates that the theory correctly predicts several features of the instability, such as stationary disturbance wavelength and orientation plus the frequency of the most highly amplified traveling wave. With regard to transition, it is found that when curvature effects are included the onset conditions are reasonably well predicted by the e^N method where N is approximately 11. The computations indicate that methods which do not include the curvature effects are unduly pessimistic for transition prediction. Finally, this study has indicated that for strongly three-dimensional flows the most highly amplified disturbances are, in general, traveling waves and not the stationary waves. It is not yet clear whether the stationary disturbances play any role in the transition process.

Acknowledgments

This work was performed at the NASA Langley Research Center, Hampton, Va., and was financed by the National Aeronautics and Space Administration under Contracts NAS1-16916 and NAS1-14605. Both authors would particularly like to thank Mr. D. M. Bushnell, Head of the Viscous Flow Branch, High Speed Aerodynamics Division, for his encouragement and enthusiastic support for the project. The second author would also like to express his thanks to the Joint Institute for the Advancement of Flight Sciences (George Washington University/NASA) for making his stay at NASA Langley possible.

References

- Hefner, J. N. and Bushnell, D. M., "An Overview of Concepts for Aircraft Drag Reduction," AGARD Rept. 654, June 1977, Paper 1.
- Jaffe, N. A., Okamura, T. T., and Smith, A. M. O., "Determination of Spatial Amplification Factors and Their Application to Transition," *AIAA Journal*, Vol. 8, Feb. 1970, pp. 301-308.
- Srokowski, A. J. and Orszag, S. A., "Mass Flow Requirements for LFC Wing Design," AIAA Paper 77-1222, Aug. 1977.
- Nayfeh, A. H., "Stability of Three-Dimensional Boundary Layers," *AIAA Journal*, Vol. 18, April 1980, pp. 406-416.
- Cebeci, T. and Stewartson, K., "On Stability and Transition of Three-Dimensional Flows," *AIAA Journal*, Vol. 18, April 1980, pp. 398-405.
- Malik, M. R. and Orszag, S. A., "Comparison of Methods for Prediction of Transition by Stability Analysis," *AIAA Journal*, Vol. 18, Dec. 1980, pp. 1485-1489.
- Hefner, J. N. and Bushnell, D. M., "Status of Linear Boundary Layer Stability Theory and the e^N Method, with Emphasis on Swept-Wing Applications," NASA TP 1645, April 1980.
- Gregory, N., Stuart, J. T., and Walker, W. S., "On the Stability of Three Dimensional Boundary Layers with Application to the Flow Due to a Rotating Disk," *Philosophical Transactions of the Royal Society of London*, Ser. A, Vol. 248, 1955, pp. 155-199.
- Malik, M. R., Wilkinson, S. P., and Orszag, S. A., "Instability and Transition in Rotating Disk Flow," *AIAA Journal*, Vol. 19, Sept. 1981, pp. 1131-1138.

¹⁰Owen, P. R. and Randall, D. G., "Boundary Layer Transition on a Swept Back Wing," Royal Aircraft Establishment, Tech. Memo. (Aero) 256, Feb. 1952.

¹¹Malik, M. R., Chuang, S., and Hussaini, M. Y., "Accurate Numerical Solutions of Compressible, Linear Stability Equations," *Zeitschrift für Angewandte Mathematik und Physik*, Vol. 33, 1982, pp. 189-201.

¹²Malik, M. R., "COSAL—A Black-Box Compressible Stability Analysis Code for Transition Prediction in Three Dimensional Boundary Layers," NASA CR 165952, 1982.

¹³Wilkinson, J. H., *The Algebraic Eigenvalue Problem*, Oxford University Press, London, 1965.

¹⁴Malik, M. R. and Orszag, S. A., "Efficient Computation of the Stability of Three-Dimensional Boundary Layers," AIAA Paper 81-1277, 1981.

¹⁵Poll, D. I. A., "Some Observations of the Transition Process on the Windward Face of a Long Yawed Cylinder," *Journal of Fluid Mechanics*, Vol. 150, Jan. 1985, pp. 329-356.

¹⁶Cebeci, T. and Kaups, K., "Compressible Laminar Boundary Layers with Suction on Swept and Tapered Wings," *Journal of Aircraft*, Vol. 14, July 1977, pp. 661-667.

¹⁷Gray, W. E., "The Nature of the Boundary Layer Flow at the Nose of a Swept Wing," Royal Aeronautical Establishment, Tech. Memo. (Aero) 256, June 1952.

From the AIAA Progress in Astronautics and Aeronautics Series...

COMBUSTION DIAGNOSTICS BY NONINTRUSIVE METHODS – v. 92

*Edited by T.D. McCay, NASA Marshall Space Flight Center
and
J.A. Roux, The University of Mississippi*

This recent Progress Series volume, treating combustion diagnostics by nonintrusive spectroscopic methods, focuses on current research and techniques finding broad acceptance as standard tools within the combustion and thermophysics research communities. This book gives a solid exposition of the state-of-the-art of two basic techniques—coherent antistokes Raman scattering (CARS) and laser-induced fluorescence (LIF)—and illustrates diagnostic capabilities in two application areas, particle and combustion diagnostics—the goals being to correctly diagnose gas and particle properties in the flowfields of interest. The need to develop nonintrusive techniques is apparent for all flow regimes, but it becomes of particular concern for the subsonic combustion flows so often of interest in thermophysics research. The volume contains scientific descriptions of the methods for making such measurements, primarily of gas temperature and pressure and particle size.

Published in 1984, 347 pp., 6 × 9, illus., \$49.50 Mem., \$69.50 List; ISBN 0-915928-86-8

TO ORDER WRITE: Publications Order Dept., AIAA, 1633 Broadway, New York, N.Y. 10019